19

Heat Transfer to Fluids at Supercritical Pressures

Igor Pioro and Sarah Mokry
University of Ontario Institute of Technology
Canada

1. Introduction

Prior to a general discussion on parametric trends in heat transfer to supercritical fluids, it is important to define special terms and expressions used at these conditions. Therefore, general definitions of selected terms and expressions, related to heat transfer to fluids at critical and supercritical pressures, are listed below. For better understanding of these terms and expressions a graph is shown in Fig. 1. General definitions of selected terms and expressions related to critical and supercritical regions are listed in the Chapter "Thermophysical Properties at Critical and Supercritical Conditions".

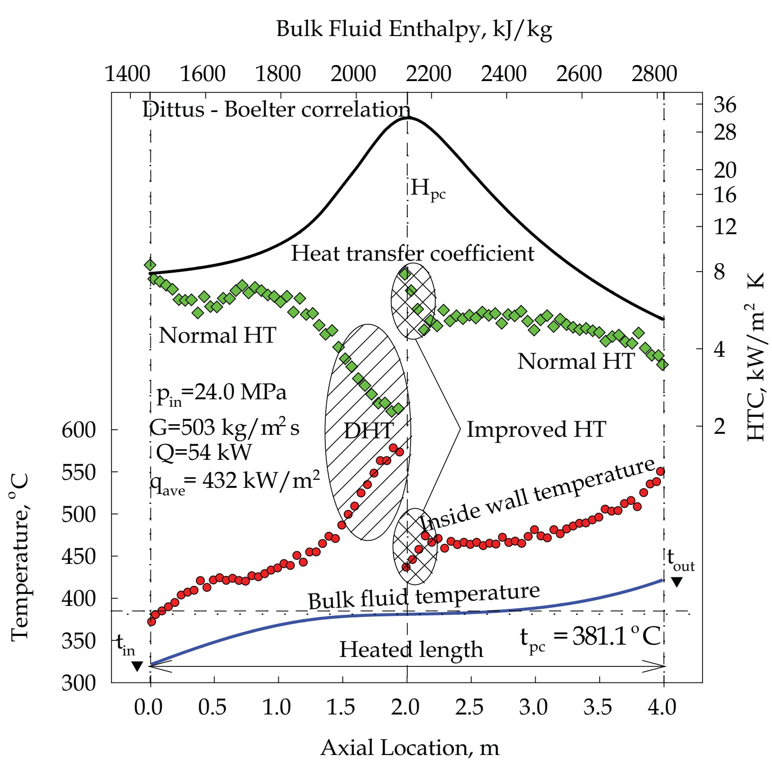

Fig. 1. Temperature and heat transfer coefficient profiles along heated length of vertical circular tube (Kirillov et al., 2003): Water, D=10 mm and L_h=4 m.

General definitions of selected terms and expressions related to heat transfer at critical and supercritical pressures

Deteriorated Heat Transfer (DHT) is characterized with lower values of the wall heat transfer coefficient compared to those at the normal heat transfer; and hence has higher values of wall temperature within some part of a test section or within the entire test section.

Improved Heat Transfer (IHT) is characterized with higher values of the wall heat transfer coefficient compared to those at the normal heat transfer; and hence lower values of wall temperature within some part of a test section or within the entire test section. In our opinion, the improved heat-transfer regime or mode includes peaks or "humps" in the heat transfer coefficient near the critical or pseudocritical points.

Normal Heat Transfer (NHT) can be characterized in general with wall heat transfer coefficients similar to those of subcritical convective heat transfer far from the critical or pseudocritical regions, when are calculated according to the conventional single-phase Dittus-Boelter-type correlations: $\mathbf{Nu} = 0.0023\ \mathbf{Re}^{0.8}\mathbf{Pr}^{0.4}$.

Pseudo-boiling is a physical phenomenon similar to subcritical pressure nucleate boiling, which may appear at supercritical pressures. Due to heating of supercritical fluid with a bulk-fluid temperature below the pseudocritical temperature (high-density fluid, i.e., "liquid"), some layers near a heating surface may attain temperatures above the pseudocritical temperature (low-density fluid, i.e., "gas") (for specifics of thermophysical properties, see Chapter "Thermophysical Properties at Critical and Supercritical Conditions"). This low-density "gas" leaves the heating surface in the form of variable density (bubble) volumes. During the pseudo-boiling, the wall heat transfer coefficient usually increases (improved heat-transfer regime).

Pseudo-film boiling is a physical phenomenon similar to subcritical-pressure film boiling, which may appear at supercritical pressures. At pseudo-film boiling, a low-density fluid (a fluid at temperatures above the pseudocritical temperature, i.e., "gas") prevents a high-density fluid (a fluid at temperatures below the pseudocritical temperature, i.e., "liquid") from contacting ("rewetting") a heated surface (for specifics of thermophysical properties, see Chapter "Thermophysical Properties at Critical and Supercritical Conditions"). Pseudo-film boiling leads to the deteriorated heat-transfer regime.

Water is the most widely used coolant or working fluid at supercritical pressures. The largest application of supercritical water is in supercritical "steam" generators and turbines, which are widely used in the power industry worldwide (Pioro and Duffey, 2007). Currently, upper limits of pressures and temperatures used in the power industry are about 30 – 35 MPa and 600 – 625°C, respectively. New direction in supercritical-water application in the power industry is a development of SuperCritical Water-cooled nuclear Reactor (SCWR) concepts, as part of the Generation-IV International Forum (GIF) initiative. However, other areas of using supercritical water exist (Pioro and Duffey, 2007).

Supercritical carbon dioxide was mostly used as a modelling fluid instead of water due to significantly lower critical parameters (for details, see Chapter "Thermophysical Properties at Critical and Supercritical Conditions"). However, currently new areas of using supercritical carbon dioxide as a coolant or working fluid have been emerged (Pioro and Duffey, 2007).

The third supercritical fluid used in some special technical applications is helium (Pioro and Duffey, 2007). Supercritical helium is used in cooling coils of superconducting electromagnets, superconducting electronics and power-transmission equipment.
Also, refrigerant R-134a is being considered as a perspective modelling fluid due to its lower critical parameters compared to those of water (Pioro and Duffey, 2007).
Experiments at supercritical pressures are very expensive and require sophisticated equipment and measuring techniques. Therefore, some of these studies (for example, heat transfer in bundles) are proprietary and hence, were not published in the open literature.
The majority of studies (Pioro and Duffey, 2007) deal with heat transfer and hydraulic resistance of working fluids, mainly water, carbon dioxide and helium, in circular bare tubes. In addition to these fluids, forced- and free-convection heat-transfer experiments were conducted at supercritical pressures, using liquefied gases such as air, argon, hydrogen; nitrogen, nitrogen tetra-oxide, oxygen and sulphur hexafluoride; alcohols such as ethanol and methanol; hydrocarbons such as n-heptane, n-hexane, di-iso-propyl-cyclo-hexane, n-octane, iso-butane, iso-pentane and n-pentane; aromatic hydrocarbons such as benzene and toluene, and poly-methyl-phenyl-siloxane; hydrocarbon coolants such as kerosene, TS-1 and RG-1, jet propulsion fuels RT and T-6; and refrigerants.
A limited number of studies were devoted to heat transfer and pressure drop in annuli, rectangular-shaped channels and bundles.
Accounting that supercritical water and carbon dioxide are the most widely used fluids and that the majority of experiments were performed in circular tubes, specifics of heat transfer and pressure drop, including generalized correlations, will be discussed in this chapter based on these conditions[1].
Specifics of thermophysical properties at critical and supercritical pressures for these fluids are discussed in the Chapter "Thermophysical Properties at Critical and Supercritical Conditions" and Pioro and Duffey (2007).

2. Convective heat transfer to fluids at supercritical pressures: Specifics of supercritical heat transfer

All[2] primary sources of heat-transfer experimental data for water and carbon dioxide flowing inside circular tubes at supercritical pressures are listed in Pioro and Duffey (2007).
In general, three major heat-transfer regimes (for their definitions, see above) can be noticed at critical and supercritical pressures (for details, see Figs. 1 and 2):
1. Normal heat transfer;
2. Improved heat transfer; and
3. Deteriorated heat transfer.

Also, two special phenomena (for their definitions, see above) may appear along a heated surface:
1. pseudo-boiling;
2. pseudo-film boiling.

[1]Specifics of heat transfer and pressure drop at other conditions and/or for other fluids are discussed in Pioro and Duffey (2007).
[2] "All" means all sources found by the authors from a total of 650 references dated mainly from 1950 till beginning of 2006.

These heat-transfer regimes and special phenomena appear to be due to significant variations of thermophysical properties near the critical and pseudocritical points (see Fig. 3) and due to operating conditions.

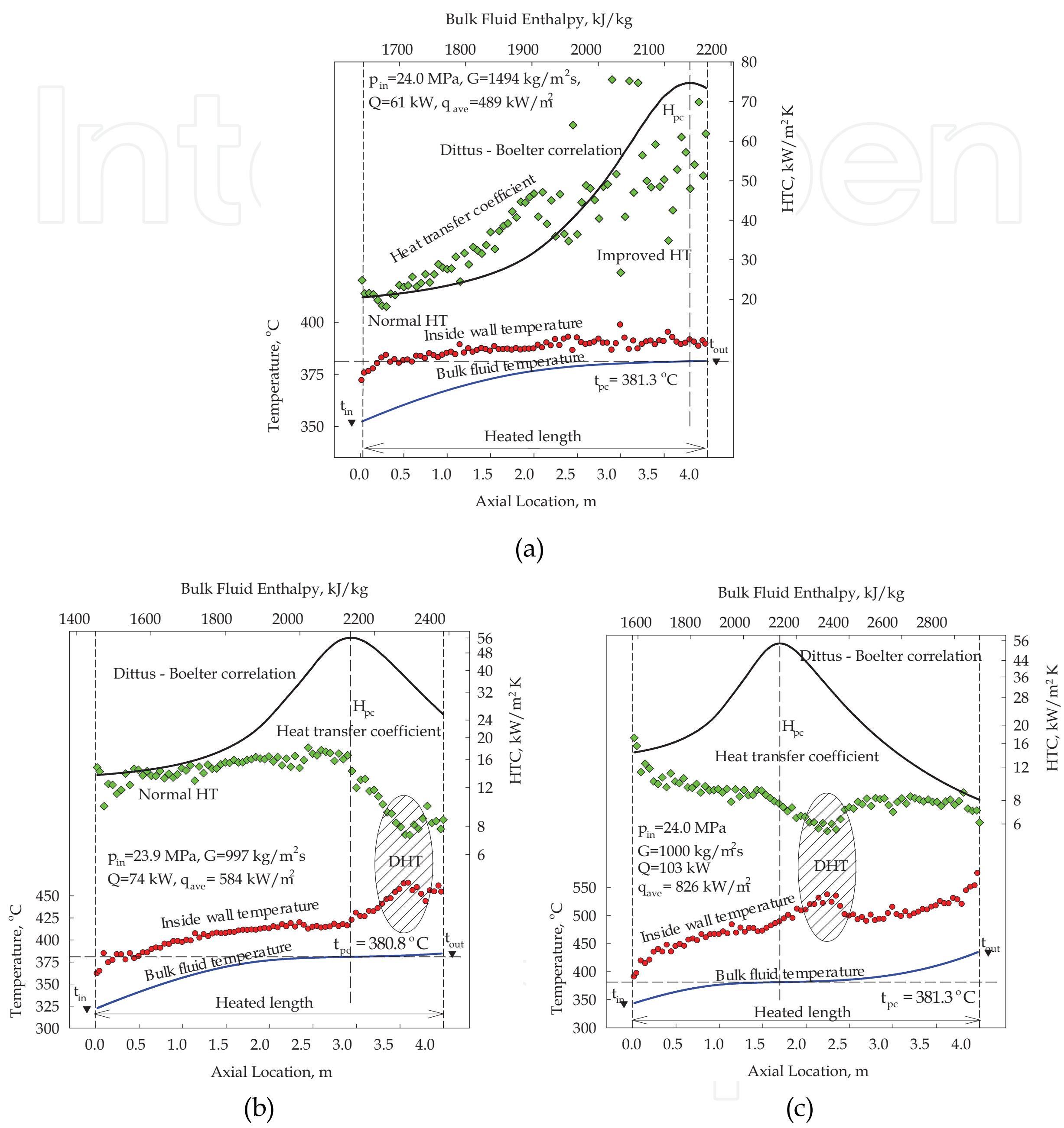

Fig. 2. Temperature and heat transfer coefficient profiles along heated length of vertical circular tube (Kirillov et al. 2003): Water, D=10 mm and L_h=4 m.

Therefore, the following cases can be distinguished at critical and supercritical pressures (for details, see Figs. 1 and 2):

a. Wall and bulk-fluid temperatures are below a pseudocritical temperature within a part or the entire heated channel;
b. Wall temperature is above and bulk-fluid temperature is below a pseudocritical temperature within a part or the entire heated channel;

c. Wall temperature and bulk fluid temperature is above a pseudocritical temperature within a part or the entire heated channel;
d. High heat fluxes;
e. Entrance region;
f. Upward and downward flows;
g. Horizontal flows;
h. Effect of gravitational forces at lower mass fluxes; etc.

All these cases can affect the supercritical heat transfer.

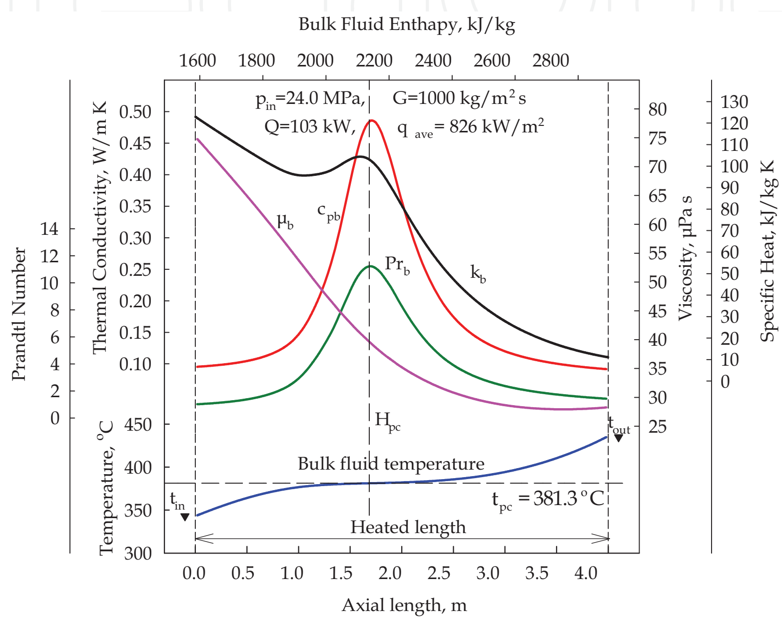

Fig. 3. Temperature and thermophysical properties profiles along heated length of vertical circular tube (operating conditions in this figure correspond to those in Fig. 2c): Water, D=10 mm and L_h=4 m; thermophysical properties based on bulk-fluid temperature.

3. Parametric trends

3.1 General heat transfer

As it was mentioned above, some researchers suggested that variations in thermophysical properties near critical and pseudocritical points resulted in the maximum value of Heat Transfer Coefficient (HTC). Thus, Yamagata et al. (1972) found that for water flowing in vertical and horizontal tubes, the HTC increases significantly within the pseudocritical region (Fig. 4). The magnitude of the peak in the HTC decreases with increasing heat flux and pressure. The maximum HTC values correspond to a bulk-fluid enthalpy, which is slightly less than the pseudocritical bulk-fluid enthalpy.

Results of Styrikovich et al. (1967) are shown in Fig. 5. Improved and deteriorated heat-transfer regimes as well as a peak (“hump”) in HTC near the pseudocritical point are clearly shown in this figure. The deteriorated heat-transfer regime appears within the middle part of the test section at a heat flux of about 640 kW/m², and it may exist together with the improved heat-transfer regime at certain conditions (also see Fig. 1). With the further heat-flux increase, the improved heat-transfer regime is eventually replaced with that of deteriorated heat transfer.

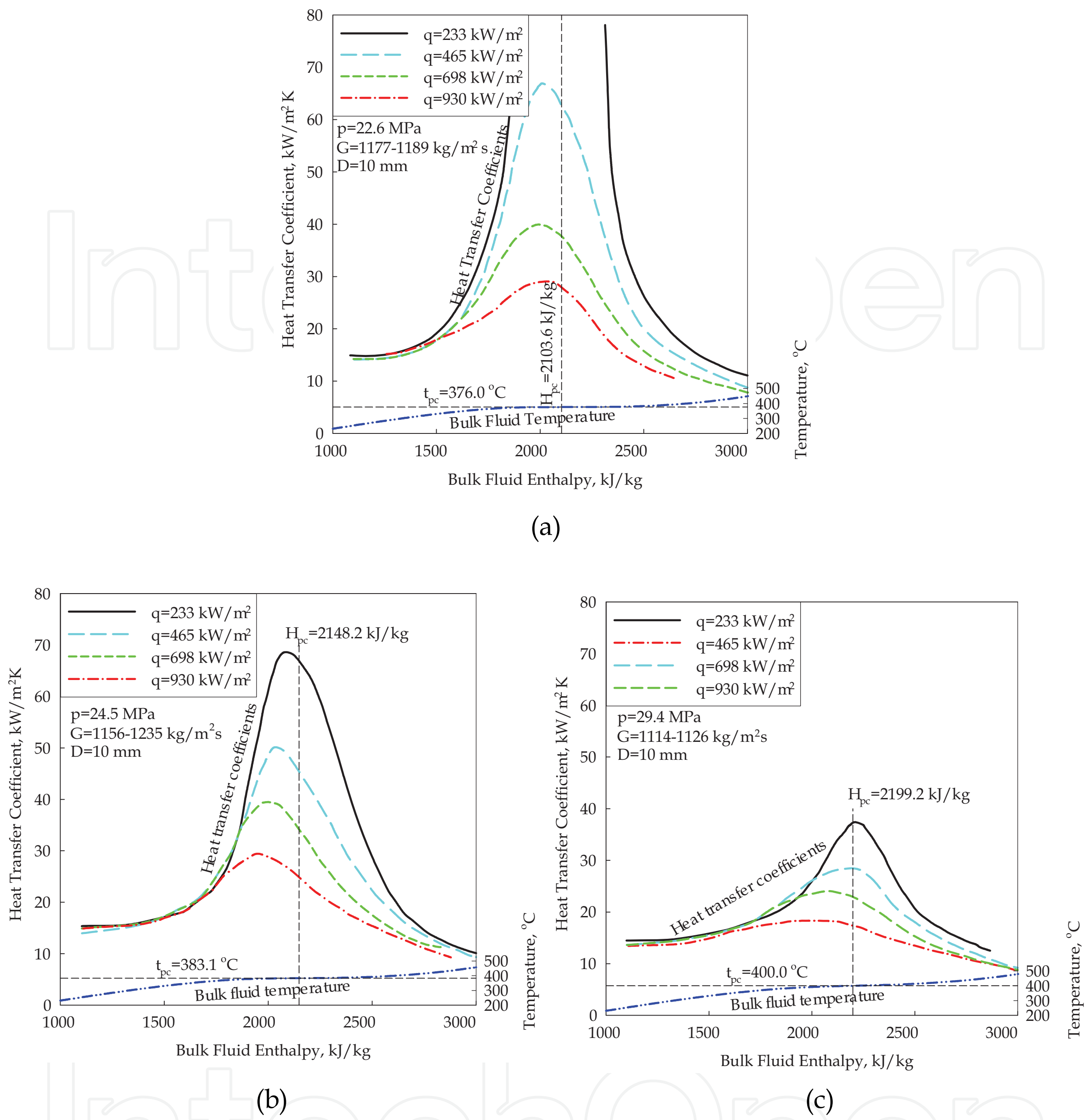

Fig. 4. Heat transfer coefficient vs. bulk-fluid enthalpy in vertical tube with upward flow at various pressures (Yamagata et al., 1972): Water – (a) p=22.6 MPa; (b) p=24.5 MPa; and (c) p=29.4 MPa.

Vikhrev et al. (1971, 1967) found that at a mass flux of 495 kg/m²s, two types of deteriorated heat transfer existed (Fig. 6): The first type appeared within the entrance region of the tube $L / D < 40 – 60$; and the second type appeared at any section of the tube, but only within a certain enthalpy range. In general, the deteriorated heat transfer occurred at high heat fluxes.

The first type of deteriorated heat transfer observed was due to the flow structure within the entrance region of the tube. However, this type of deteriorated heat transfer occurred mainly at low mass fluxes and at high heat fluxes (Fig. 6a,b) and eventually disappeared at high mass fluxes (Fig. 6c,d).

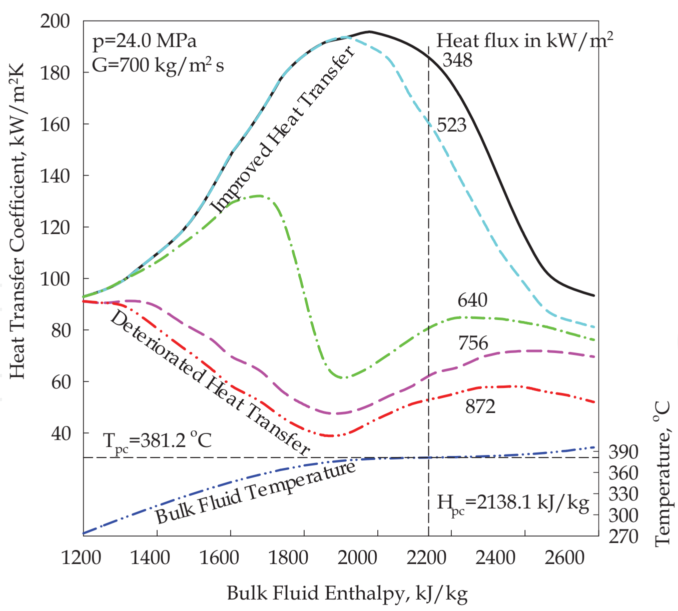

Fig. 5. Variations in heat transfer coefficient values of water flowing in tube (Styrikovich et al., 1967).

The second type of deteriorated heat transfer occurred when the wall temperature exceeded the pseudocritical temperature (Fig. 6). According to Vikhrev et al. (1967), the deteriorated heat transfer appeared when q / G > 0.4 kJ/kg (where q is in kW/m² and G is in kg/m²s). This value is close to that suggested by Styrikovich et al. (1967) (q / G > 0.49 kJ/kg). However, the above-mentioned definitions of two types of deteriorated heat transfer are not enough for their clear identification.

3.2 Pseudo-boiling and pseudo-film boiling phenomena

Ackerman (1970) investigated heat transfer to water at supercritical pressures flowing in smooth vertical tubes with and without internal ribs within a wide range of pressures, mass fluxes, heat fluxes and diameters. He found that pseudo-boiling phenomenon could occur at supercritical pressures. The pseudo-boiling phenomenon is thought to be due to large differences in fluid density below the pseudocritical point (high-density fluid, i.e., “liquid”) and beyond (low-density fluid, i.e., “gas”). This heat-transfer phenomenon was affected with pressure, bulk-fluid temperature, mass flux, heat flux and tube diameter.

The process of pseudo-film boiling (i.e., low-density fluid prevents high-density fluid from “rewetting” a heated surface) is similar to film boiling, which occurs at subcritical pressures. Pseudo-film boiling leads to the deteriorated heat transfer. However, the pseudo-film boiling phenomenon may not be the only reason for deteriorated heat transfer. Ackerman noted that unpredictable heat-transfer performance was sometimes observed when the pseudocritical temperature of the fluid was between the bulk-fluid temperature and the heated surface temperature.

Kafengaus (1986, 1975), while analyzing data of various fluids (water, ethyl and methyl alcohols, heptane, etc.), suggested a mechanism for “pseudo-boiling” that accompanies heat transfer to liquids flowing in small-diameter tubes at supercritical pressures. The onset of pseudo-boiling was assumed to be associated with the breakdown of a low-density wall layer that was present at an above-pseudocritical temperature, and with the entrainment of individual volumes of the low-density fluid into the cooler (below pseudocritical temperature) core of the high-density flow, where these low-density volumes collapse with the generation of pressure pulses. At certain conditions, the frequency of these pulses can coincide with the frequency of the fluid column in the tube, resulting in resonance and in a rapid rise in the amplitude of pressure fluctuations. This theory was supported with experimental results.

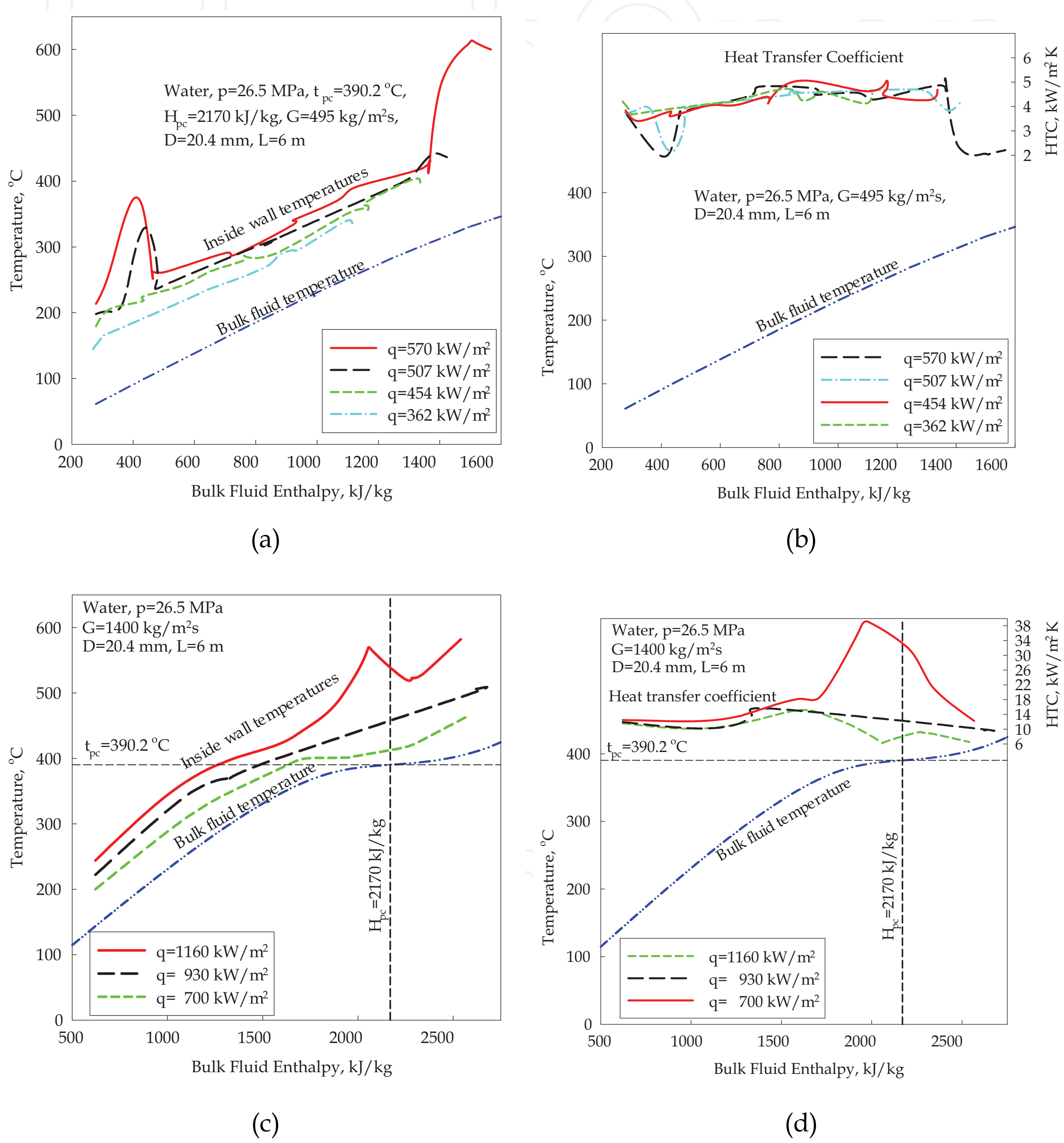

Fig. 6. Temperature profiles (a) and (c) and HTC values (b) and (d) along heated length of a vertical tube (Vikhrev et al., 1967): HTC values were calculated by the authors of the current chapter using the data from the corresponding figure; several test series were combined in each curve in figures (c) and (d).

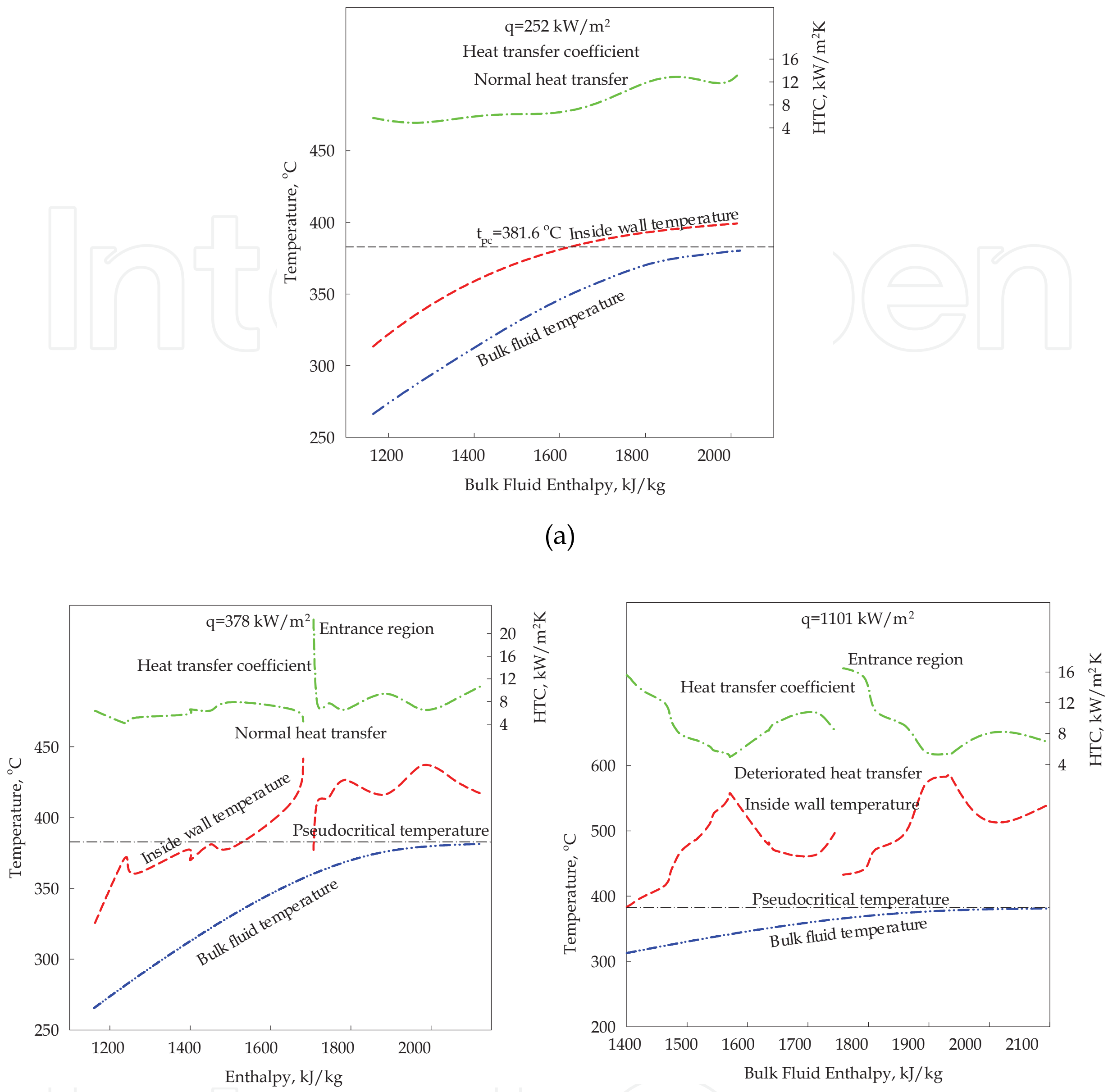

(b) (c)

Fig. 7. Temperature and heat transfer coefficient profiles along 38.1-mm ID smooth vertical tube at different mass fluxes (Lee and Haller, 1974): Water, p=24.1 MPa, and H_{pc}=2140 kJ/kg; (a) G=542 kg/m²s, (b) G=542 kg/m²s, and (c) G=1627 kg/m²s; HTC values were calculated by the authors of the current chapter using data from the corresponding figure; several test series were combined in each curve.

3.3 Horizontal flows

All[3] primary sources of experimental data for heat transfer to water and carbon dioxide flowing in horizontal test sections are listed in Pioro and Duffey (2007).

[3] "All" means all sources found by the authors from a total of 650 references dated mainly from 1950 till beginning of 2006.

Krasyakova et al. (1967) found that in a horizontal tube, in addition to the effects of non-isothermal flow that is relevant to a vertical tube, the effect of gravitational forces is important. The latter effect leads to the appearance of temperature differences between the lower and upper parts of the tube. These temperature differences depend on flow enthalpy, mass flux and heat flux. A temperature difference in a tube cross section was found at G = 300 – 1000 kg/m^{2}s and within the investigated range of enthalpies (H_b = 840 – 2520 kJ/kg). The temperature difference was directly proportional to increases in heat-flux values. The effect of mass flux on the temperature difference is the opposite, i.e., with increase in mass flux the temperature difference decreases. Deteriorated heat transfer was also observed in a horizontal tube. However, the temperature profile for a horizontal tube at locations of deteriorated heat transfer differs from that for a vertical tube, being smoother for a horizontal tube compared to that of a vertical tube with a higher temperature increase on the upper part of the tube than on the lower part.

3.4 Heat-transfer enhancement

Similar to subcritical pressures, turbulization of flow usually leads to heat-transfer enhancement at supercritical pressures.

Shiralkar and Griffith (1970) determined both theoretically (for supercritical water) and experimentally (for supercritical carbon dioxide) the limits for safe operation, in terms of the maximum heat flux for a particular mass flux. Their experiments with a twisted tape inserted inside a test section showed that heat transfer was improved by this method. Also, they found that at high heat fluxes deteriorated heat transfer occurred when the bulk-fluid temperature was below and the wall temperature was above the pseudocritical temperature.

Findings of Lee and Haller (1974) are shown in Fig. 7. They combined several test series into one graph. Due to the deteriorated heat-transfer region at the tube exit (one set of data) and the entrance effect in another set of data, experimental curves discontinue (see Fig. 7b,c). In general, they found heat flux and tube diameter to be the important parameters affecting minimum mass-flux limits to prevent pseudo-film boiling. Multi-lead ribbed tubes were found to be effective in preventing pseudo-film boiling.

3.5 Heat transfer in bundles

SCWRs will be cooled with a light-water coolant at a pressure of about 25 MPa and within a range of temperatures from 280 – 350°C to 550 – 625°C (inlet and outlet temperatures). Performing experiments at these conditions and bundle flow geometry is very complicated and expensive task. Therefore, currently preliminary experiments are performed in modelling fluids such as carbon dioxide and Freons (Richards et al., 2010). Their thermophysical properties are well known within a wide range of conditions, including the supercritical-pressure region (for details, see in Pioro and Duffey (2007) and in Chapter "Thermophysical Properties at Critical and Supercritical Conditions").

Experimental data obtained in a bare bundle with 7 circular elements, installed in a hexagonal flow channel located inside a ceramic insert surrounded by a pressure tube (Fig. 8) and cooled with R-12, are shown in Fig. 9 for reference purposes. The bundle has a 6 + 1 bare-element arrangement with each element being held at the ends to eliminate the use of spacers. Each of the 7 heating elements has a 9.5-mm outer diameter, and they are spaced one from another with a pitch of 11.29 mm. The total flow area is 374.0 mm^2, wetted perimeter – 318.7 mm, and hydraulic-equivalent diameter – 4.69 mm.

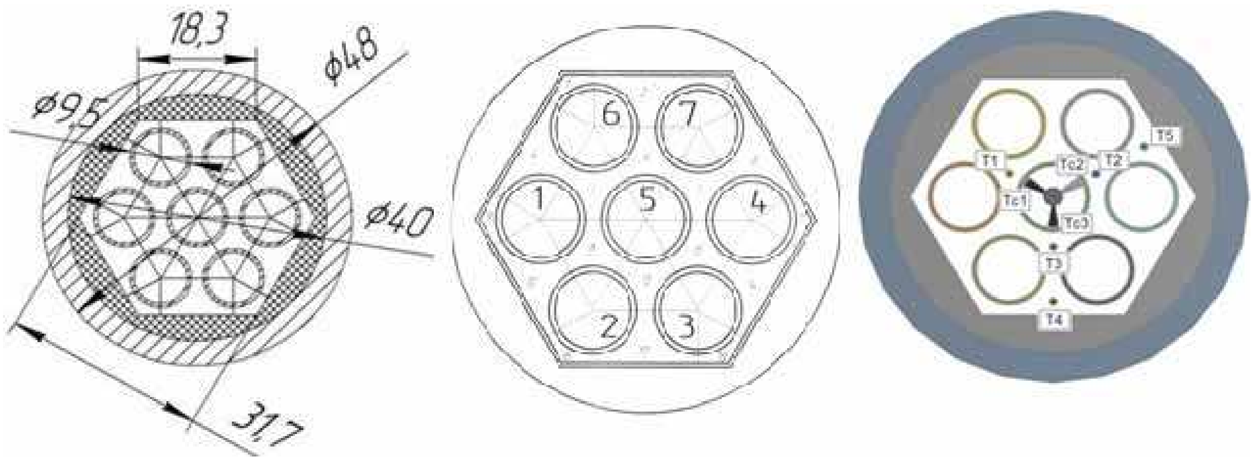

(a) (b) (c)

Fig. 8. Flow-channel cross sections: (a) with dimensions; (b) with elements numbering, and (c) with thermocouple layout.

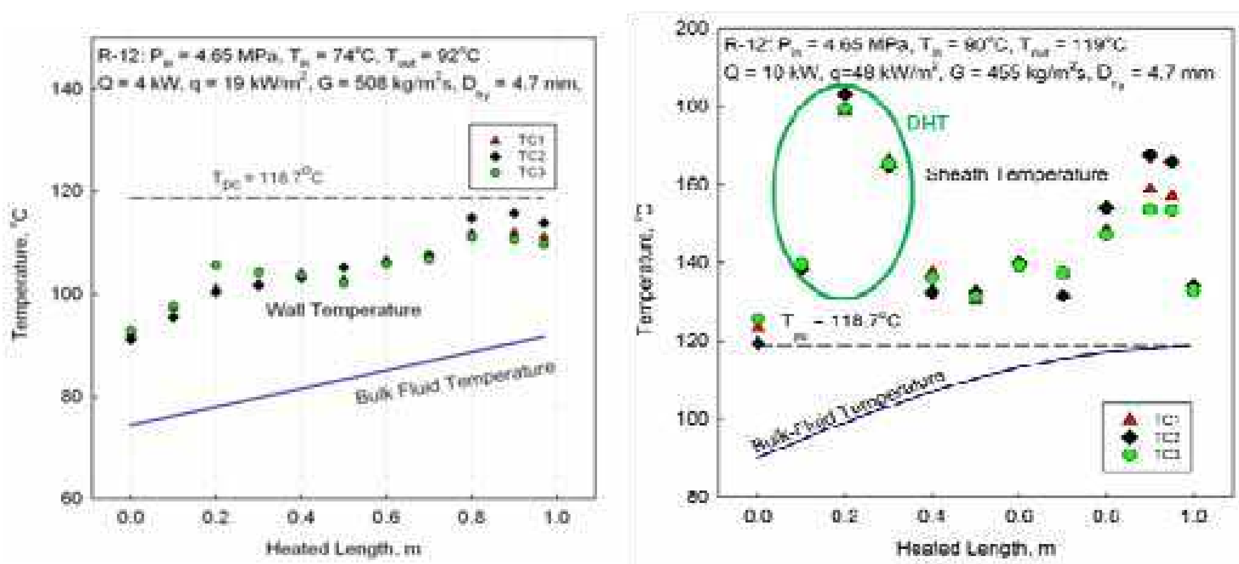

(a) (b)

Fig. 9. Bulk-fluid and sheath-temperature profiles along bundle heated length: (a) normal heat-transfer regime; and (b) normal and deteriorated heat-transfer regimes.

The main test-section components are cylindrical heated elements installed tightly in the vertical hexagonal shell (downward flow). The entire internal setup is contained by a cylindrical 40 × 4 mm pressure tube with welded flanges at the edges that form the upper (inlet) chamber and lower (outlet) chamber, with a total heated length of 1000 mm. Four thermocouples installed into the top and bottom chambers were used to measure Freon-12 inlet and outlet temperatures. Basic parameters of the experimental setup are listed in Table 1.

The experiments showed that at certain operating conditions the deteriorated heat-transfer regime is possible not only in bare tubes, but also in "bare" bundles. This is the important statement, because previously deteriorated heat-transfer regimes have not been encountered in supercritical water-cooled bundles with helical fins (Pioro and Duffey, 2007).

Pressure	Up to 5.0 MPa (equivalent to 25.5 MPa for water)
Temperature of Freon-12	Up to 120°C (400°C heating elements)
Maximum flow rate	20 + 20 m^3/h
Maximum pump pressure head	1.0 + 1.0 MPa
Experimental test-section power	Up to 1 MW
Experimental test-section height	Up to 8 m
Data Acquisition System (DAS)	Up to 256 channels

Table 1. Main parameters of 7-element bare bundle cooled with R-12.

4. Practical prediction methods for convection heat transfer at supercritical pressures

4.1 Circular vertical tubes

Unfortunately, satisfactory analytical methods have not yet been developed due to the difficulty in dealing with steep property variations, especially, in turbulent flows and at high heat fluxes. Therefore, generalized correlations based on experimental data are used for HTC calculations at supercritical pressures.

There are a lot of various correlations for convection heat transfer in circular tubes at supercritical pressures (for details, see in Pioro and Duffey (2007)). However, an analysis of these correlations showed that they are more or less accurate only within a particular dataset, which was used to derive the correlation, but show a significant deviation in predicting other experimental data. Therefore, only selected correlations are listed below.

In general, many of these correlations are based on the conventional Dittus-Boelter-type correlation (see Eq. (1)) in which the regular specific heat is replaced with the cross-section averaged specific heat within the range of (T_w – T_b); $\left(\frac{H_w - H_b}{T_w - T_b}\right)$, J/kg K (see Fig. 8). Also, additional terms, such as: $\left(\frac{k_b}{k_w}\right)^k$; $\left(\frac{\mu_b}{\mu_w}\right)^m$; $\left(\frac{\rho_b}{\rho_w}\right)^n$; etc., can be added into correlations to account for significant variations in thermophysical properties within a cross section, due to a non-uniform temperature profile, i.e., due to heat flux.

It should be noted that usually generalized correlations, which contain fluid properties at the wall temperature, require iterations to be solved, because there are two unknowns: 1) HTC and 2) the corresponding wall temperature. Therefore, the initial wall-temperature value at which fluid properties will be estimated should be "guessed" to start iterations.

The most widely used heat-transfer correlation at subcritical pressures for forced convection is the Dittus-Boelter (1930) correlation (Pioro and Duffey, 2007). In 1942, McAdams proposed to use the Dittus-Boelter correlation in the following form, for forced-convective heat transfer in turbulent flows at subcritical pressures:

$$\mathrm{Nu_b} = 0.0243\,\mathrm{Re_b^{0.8}}\mathrm{Pr_b^{0.4}}\,. \tag{1}$$

However, it was noted that Eq. (1) might produce unrealistic results within some flow conditions (see Figs. 1 and 2), especially, near the critical and pseudocritical points, because it is very sensitive to properties variations.

In general, experimental heat transfer coefficient values show just a moderate increase within the pseudocritical region. This increase depends on flow conditions and heat flux:

higher heat flux – less increase. Thus, the bulk-fluid temperature might not be the best characteristic temperature at which all thermophysical properties should be evaluated. Therefore, the cross-sectional averaged Prandtl number (see below), which accounts for thermophysical properties variations within a cross section due to heat flux, was proposed to be used in many supercritical heat-transfer correlations instead of the regular Prandtl number. Nevertheless, this classical correlation (Eq. (1)) was used extensively as a basis for various supercritical heat-transfer correlations.

In 1964, Bishop et al. conducted experiments in supercritical water flowing upward inside bare tubes and annuli within the following range of operating parameters: P=22.8 – 27.6 MPa, T_b= 282 – 527ºC, G = 651 – 3662 kg/m²s and q = 0.31 – 3.46 MW/m². Their data for heat transfer in tubes were generalized using the following correlation with a fit of ±15%:

$$\mathrm{Nu}_b = 0.0069\,\mathrm{Re}_b^{0.9}\,\overline{\mathrm{Pr}}_b^{0.66}\left(\frac{\rho_w}{\rho_b}\right)^{0.43}\left(1+2.4\frac{D}{x}\right). \tag{2}$$

Equation (2) uses the cross-sectional averaged Prandtl number, and the last term in the correlation: (1+2.4 D/x), accounts for the entrance-region effect. However, in the present comparison, the Bishop et al. correlation was used without the entrance-region term as the other correlations (see Eqs. (1), (3) and (4)).

In 1965, Swenson et al. found that conventional correlations, which use a bulk-fluid temperature as a basis for calculating the majority of thermophysical properties, were not always accurate. They have suggested the following correlation in which the majority of thermophysical properties are based on a wall temperature:

$$\mathrm{Nu}_\mathrm{w} = 0.00459\,\mathrm{Re}_\mathrm{w}^{0.923}\,\overline{\mathrm{Pr}}_\mathrm{w}^{0.613}\left(\frac{\rho_w}{\rho_b}\right)^{0.231}. \tag{3}$$

Equation (3) was obtained within the following range: pressure 22.8 − 41.4 MPa, bulk-fluid temperature 75 − 576ºC, wall temperature 93 − 649ºC and mass flux 542 − 2150 kg/m²s; and predicts experimental data within ±15%.

In 2002, Jackson modified the original correlation of Krasnoshchekov et al. from 1967 for forced-convective heat transfer in water and carbon dioxide at supercritical pressures, to employ the Dittus-Boelter-type form for $\mathbf{Nu}_0$ as the following:

$$\mathrm{Nu}_\mathrm{b} = 0.0183\,\mathrm{Re}_\mathrm{b}^{0.82}\,\mathrm{Pr}_\mathrm{b}^{0.5}\left(\frac{\rho_w}{\rho_b}\right)^{0.3}\left(\frac{\bar{c}_p}{c_{pb}}\right)^{n}, \tag{4}$$

where the exponent n is defined as following:

$n = 0.4$ for $T_b < T_w < T_{pc}$ and for $1.2\,T_{pc} < T_b < T_w$;

$n = 0.4 + 0.2\left(\frac{T_w}{T_{pc}} - 1\right)$ for $T_b < T_{pc} < T_w$; and

$n = 0.4 + 0.2\left(\frac{T_w}{T_{pc}} - 1\right)\left[1 - 5\left(\frac{T_b}{T_{pc}} - 1\right)\right]$ for $T_{pc} < T_b < 1.2\,T_{pc}$ and $T_b < T_w$.

An analysis performed by Pioro and Duffey (2007) showed that the two following correlations: 1) Bishop et al. (1964) and 2) Swenson et al. (1965); were obtained within the same range of operating conditions as those for SCWRs.

The majority of empirical correlations were proposed in the 1960s – 1970s, when experimental techniques were not at the same level (i.e., advanced level) as they are today. Also, thermophysical properties of water have been updated since that time (for example, a peak in thermal conductivity in critical and pseudocritical points within a range of pressures from 22.1 to 25 MPa was not officially recognized until the 1990s).

Therefore, recently a new or an updated correlation, based on a new set of heat-transfer data and the latest thermophysical properties of water (NIST, 2007) within the SCWRs operating range, was developed and evaluated (Mokry et al., 2009):

$$\mathrm{Nu_b} = 0.0061\, \mathrm{Re_b^{0.904}}\, \overline{\mathrm{Pr}}_\mathrm{b}^{0.684} \left(\frac{\rho_w}{\rho_b}\right)^{0.564}. \tag{5}$$

Figure 10 shows scatter plots of experimental HTC values versus calculated HTC values according to Eq. (5), and calculated and experimental values for wall temperatures. Both plots lie along a 45-degree straight line with an experimental data spread of ±25% for the HTC values and ±15% for the wall temperatures.

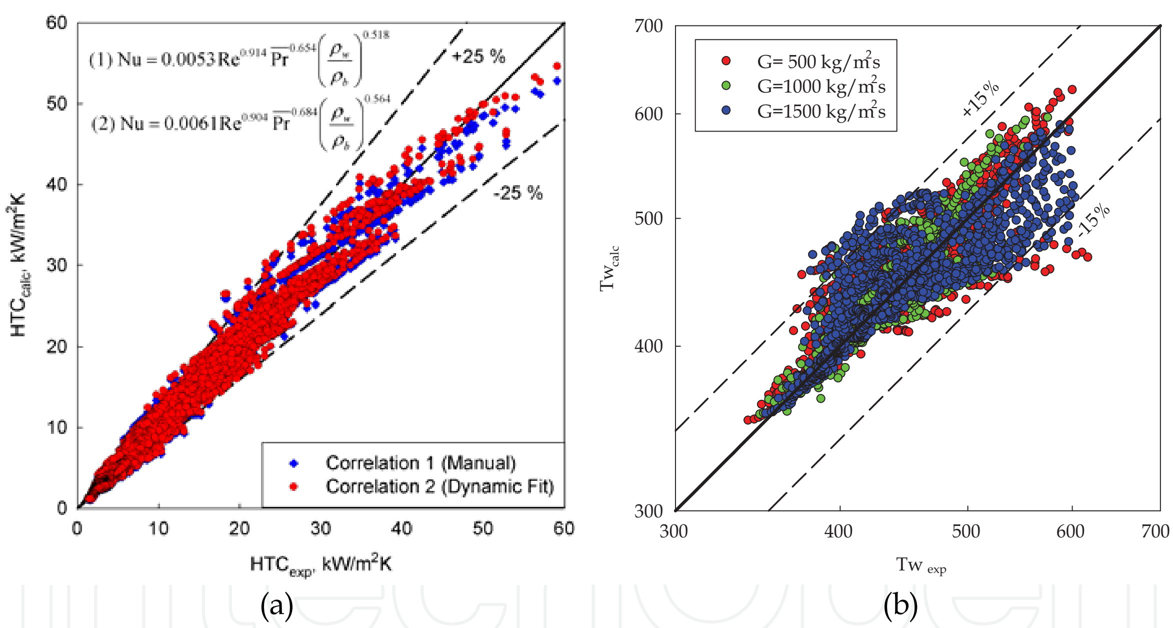

Fig. 10. Comparison of data fit through Eq. (5) with experimental data: (a) for HTC and (b) for wall temperature.

Figures 11 and 12 show a comparison of Eq. (5) with the experimental data. Figure 13 shows a comparison between experimentally obtained HTC and wall-temperature values and those calculated with FLUENT CFD code and Eq. (5).

It should be noted that all heat-transfer correlations presented in this chapter are intended only for the normal and improved heat-transfer regimes.

The following empirical correlation was proposed for calculating the minimum heat flux at which the deteriorated heat-transfer regime appears:

$$q_{dht} = -58.97 + 0.745 \cdot G\text{, kW/m}^2. \tag{6}$$

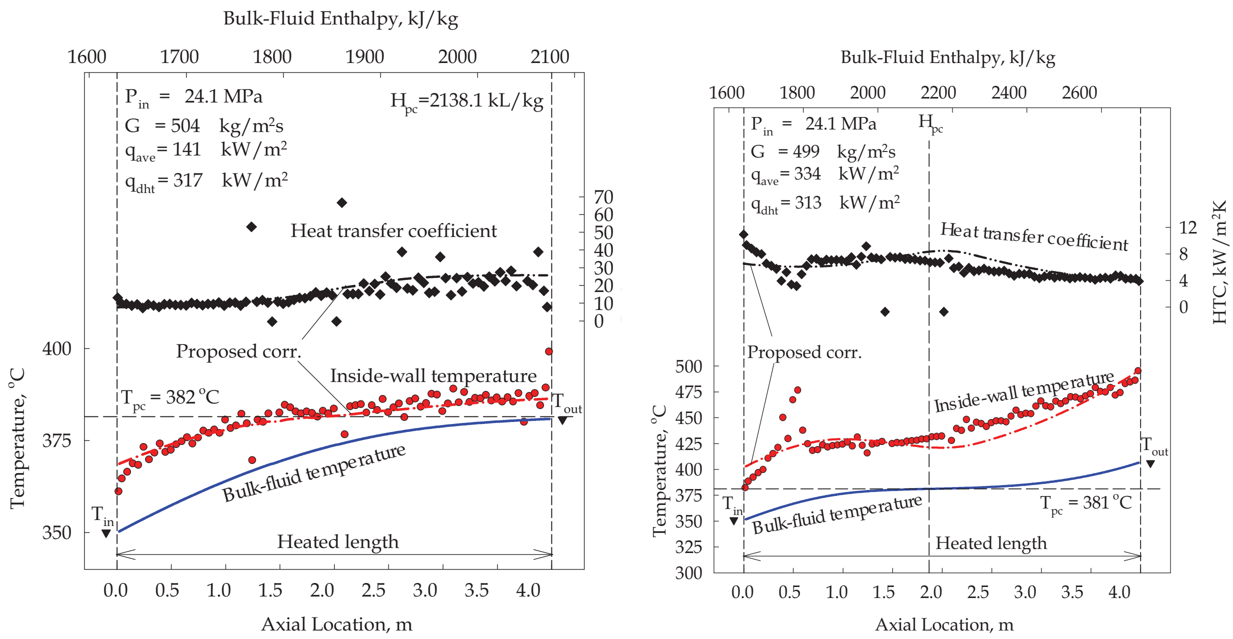

(a) (b)

Fig. 11. Temperature and HTC profiles at various heat fluxes along 4-m circular tube (D=10 mm): P_{in}=24.1 MPa and G=500 kg/m²s; "proposed correlation" – Eq. (5).

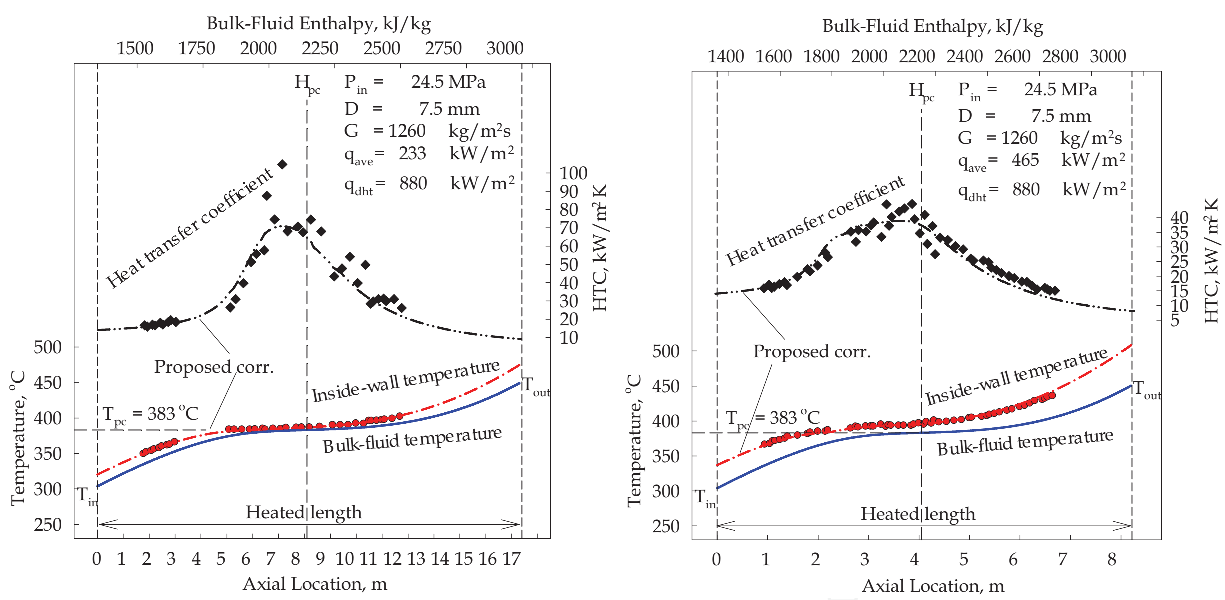

(a) (b)

Fig. 12. Temperature and HTC profiles along circular tube at various heat fluxes: Nominal operating conditions – P_{in}=24.5 MPa and D=7.5 mm (Yamagata et al., 1972); "proposed correlation" – Eq. (5).

Figures 11 – 13 show that the latest correlation (Eq. (5)) closely represents experimental data and follows trends closely even within the pseudocritical range. CFD codes are nice and a modern approach. However, not all turbulent models are applicable to heat transfer at supercritical pressures, plus these codes should be tuned first on the basis of experimental data and after that used in similar calculations.

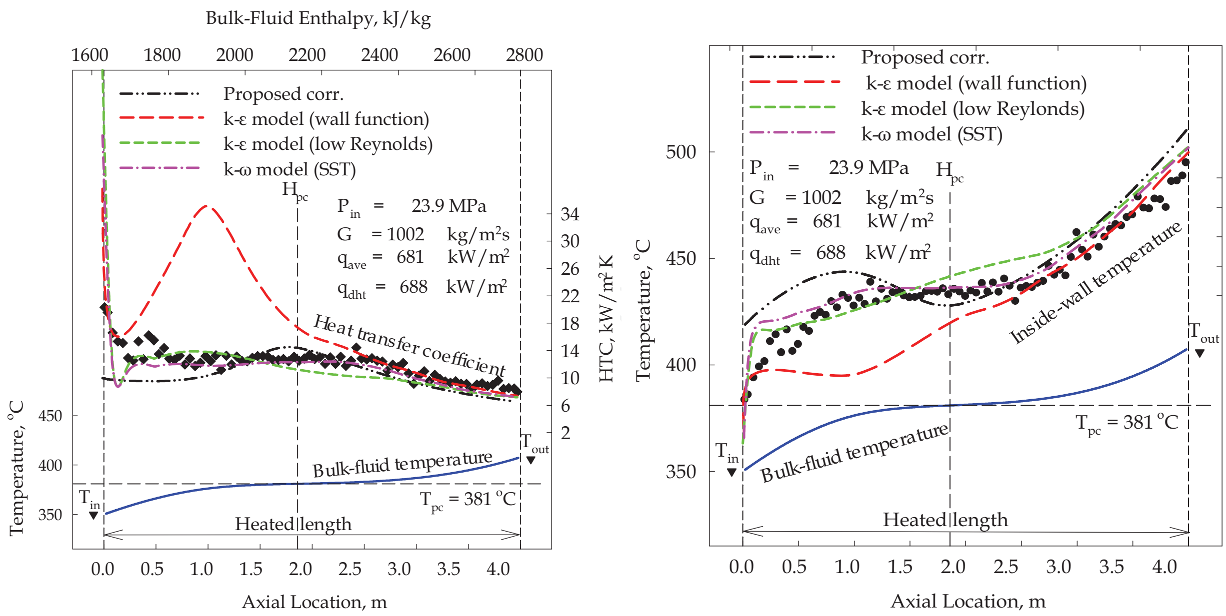

(a) (b)

Fig. 13. Comparison of HTC and wall temperature values calculated with proposed correlation (Eq. (5)) and FLUENT CFD-code (Vanyukova et al., 2009) with experimental data along 4-m circular tube (D=10 mm): P_{in}=23.9 MPa and G=1000 kg/m²s.

Correlation*	Supercritical Region				Region	
	Liquid-Like		Gas-Like		Critical or Pseudocritical	
	Errors, %					
	Average	RMS	Average	RMS	Average	RMS
Bishop et al. (1965)	6.3	24.2	5.2	18.4	20.9	28.9
Swenson et al. (1965)	1.5	25.2	-15.9	20.4	5.1	23.0
Krasnoshchekov et al. (1967)	15.2	33.7	-33.6	35.8	25.2	61.6
Watts & Chou (1982)	4.0	25.0	-9.7	20.8	5.5	24.0
Chou (1982)	5.5	23.1	5.7	22.2	16.5	28.4
Griem (1996)	1.7	23.2	4.1	22.8	2.7	31.1
Jackson (2002)	13.5	30.1	11.5	28.7	22.0	40.6
Mokry et al. (2009)	-3.9	**21.3**	-8.5	**16.5**	**-2.3**	**17.0**
Kuang et al. (2008)	-6.6	23.7	**2.9**	19.2	-9.0	24.1
Cheng et al. (2009)	**1.3**	25.6	**2.9**	28.8	14.9	90.6
Hadaller & Benerjee (1969)	7.6	30.5	10.7	20.5	-	-
Sieder & Tate (1936)	20.8	37.3	93.2	133.6	-	-
Dittus & Boelter (1930)	32.5	46.7	87.7	131.0	-	-
Gnielinski (1976)	42.5	57.6	106.3	153.3	-	-

In bold – the minimum values.
* many of these correlations can be found in Pioro and Duffey (2007).

Table 2. Overall weighted average and RMS errors within three supercritical sub-regions (Zahlan et al., 2010).

A recent study was conducted by Zahlan et al. (2010) in order to develop a heat-transfer look-up table for the critical/supercritical pressures. An extensive literature review was conducted, which included 28 datasets and 6663 trans-critical heat-transfer data. Tables 2 and 3 list results of this study in the form of the overall-weighted average and Root-Mean-Square (RMS) errors: (a) Within three supercritical sub-regions for many heat-transfer correlations, including those discussed in this chapter (Table 2); and (b) For subcritical liquid and superheated steam (Table 3). In their conclusions, Zahlan et al. (2010) determined that within the supercritical region the latest correlation by Mokry et al. (Eq. (5)) showed the best prediction for the data within all three sub-regions investigated. Also, the Mokry et al. correlation showed quite good predictions for subcritical liquid and superheated steam compared to other several correlations.

Correlation	**Subcritical liquid**		**Superheated steam**	
	Error, %			
	Average	**RMS**	**Average**	**RMS**
Sieder & Tate (1936)	27.6	37.4	83.8	137.8
Gnielinski (1976)	-4.3	**18.3**	80.3	130.2
Hadaller & Banerjee (1969)	27.3	35.9	19.1	34.4
Dittus & Boelter (1930)	10.4	22.5	75.3	127.3
Mokry et al. (2009)	**-1.1**	19.2	**-4.8**	**19.6**

In bold – the minimum values.

Table 3. Overall average and RMS error within subcritical region (Zahlan et al., 2010).

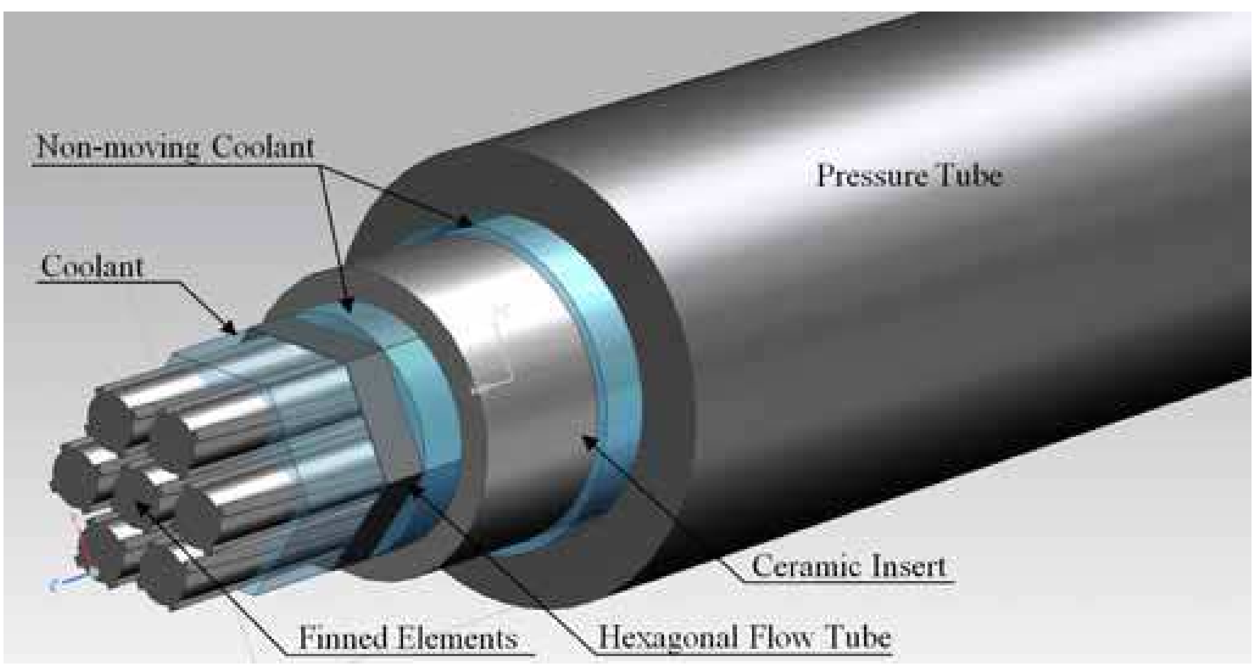

Fig. 14. Tested 7-element helically-finned bundle cooled with supercritical water and heated with electrical current (drawing prepared by W. Peiman, UOIT).

4.2 Bundles

As it was mentioned above, experiments in bundles cooled with supercritical water are very complicated and expensive. Therefore, only one empirical correlation is known so far in the open literature which predicts heat transfer coefficients in a special bundle design (Fig. 14). This correlation was developed by Dyadyakin and Popov (1977), who performed experiments in a tight 7-rod bundle with helical fins cooled with supercritical water. They have correlated their data for the local heat transfer coefficients as:

$$\mathrm{Nu_x} = 0.021\,\mathrm{Re_x^{0.8}}\,\overline{\mathrm{Pr}}_\mathrm{x}^{0.7}\left(\frac{\rho_w}{\rho_b}\right)_x^{0.45}\left(\frac{\mu_b}{\mu_{in}}\right)_x^{0.2}\left(\frac{\rho_b}{\rho_{in}}\right)_x^{0.1}\left(1+2.5\frac{D_{hy}}{x}\right), \tag{9}$$

where x is the axial location along the heated length in meters, and D_{hy} is the hydraulic-equivalent diameter (equals 4 times the flow area divided by the wetted perimeter) in meters. This correlation fits the data (504 points) to within ±20%. The maximum deviation of the experimental data from the correlating curve corresponds to points with small temperature differences between the wall temperature and bulk temperature. Sixteen experimental points had deviations from the correlation within ±30%.

5. Hydraulic resistance

In general, the total pressure drop for forced convection flow inside a test section, installed in a closed-loop system, can be calculated according to the following expression:

$$\Delta p = \sum \Delta p_{fr} + \sum \Delta p_{\ell} + \sum \Delta p_{ac} + \sum \Delta p_g\,, \tag{10}$$

where Δp is the total pressure drop, Pa.
Δp_{fr} is the pressure drop due to frictional resistance (Pa), which defined as

$$\Delta p_{fr} = \left(\xi_{fr}\frac{L}{D}\frac{\rho u^2}{2}\right) = \left(\xi_{fr}\frac{L}{D}\frac{G^2}{2\rho}\right), \tag{11}$$

where ξ_{fr} is the frictional coefficient, which can be obtained from appropriate correlations for different flow geometries. For smooth circular tubes ξ_{fr} is as follows (Filonenko, 1954)

$$\xi_{fr} = \left(\frac{1}{(1.82\log_{10}\mathrm{Re_b} - 1.64)^2}\right). \tag{12}$$

Equation (12) is valid within a range of **Re** = $4\cdot10^3 - 10^{12}$.
Usually, thermophysical properties and the Reynolds number in Eqs. (11) and (12) are based on arithmetic average of inlet and outlet values.
Δp_{ℓ} is the pressure drop due to local flow obstruction (Pa), which is defined as

$$\Delta p_{\ell} = \left(\xi_{\ell}\frac{\rho u^2}{2}\right) = \left(\xi_{\ell}\frac{G^2}{2\rho}\right), \tag{13}$$

where ξ_ℓ is the local resistance coefficient, which can be obtained from appropriate correlations for different flow obstructions.
Δp_{ac} is the pressure drop due to acceleration of flow (Pa) defined as

$$\Delta p_{ac} = \left(\rho_{out}\, u_{out}^2 - \rho_{in}\, u_{in}^2\right) = G^2 \left(\frac{1}{\rho_{out}} - \frac{1}{\rho_{in}}\right). \tag{14}$$

Δp_g is the pressure drop due to gravity (Pa) defined as

$$\Delta p_g = \pm g \left(\frac{\rho_{out} + \rho_{in}}{2}\right) L \sin\theta\,, \tag{15}$$

where θ is the test-section inclination angle to the horizontal plane, sign "+" is for the upward flow and sign "–" is for the downward flow. The arithmetic average value of densities can be used only for short sections in the case of strongly non-linear dependency of the density versus temperature. Therefore, in long test sections at high heat fluxes and within the critical and pseudocritical regions, the integral value of densities should be used (see Eq. (16)).
Ornatskiy et al. (1980) and Razumovskiy (2003) proposed to calculate Δp_g at supercritical pressures as the following:

$$\Delta p_g = \pm g \left(\frac{H_{out}\, \rho_{out} + H_{in}\, \rho_{in}}{H_{out} + H_{in}}\right) L \sin\theta\,. \tag{16}$$

In general, Equation (10) is applicable for subcritical and supercritical pressures. However, adjustment of this expression to conditions of supercritical pressures, with single-phase dense gas and significant variations in thermophysical properties near the critical and pseudocritical points, was the major task for the researchers and scientists.

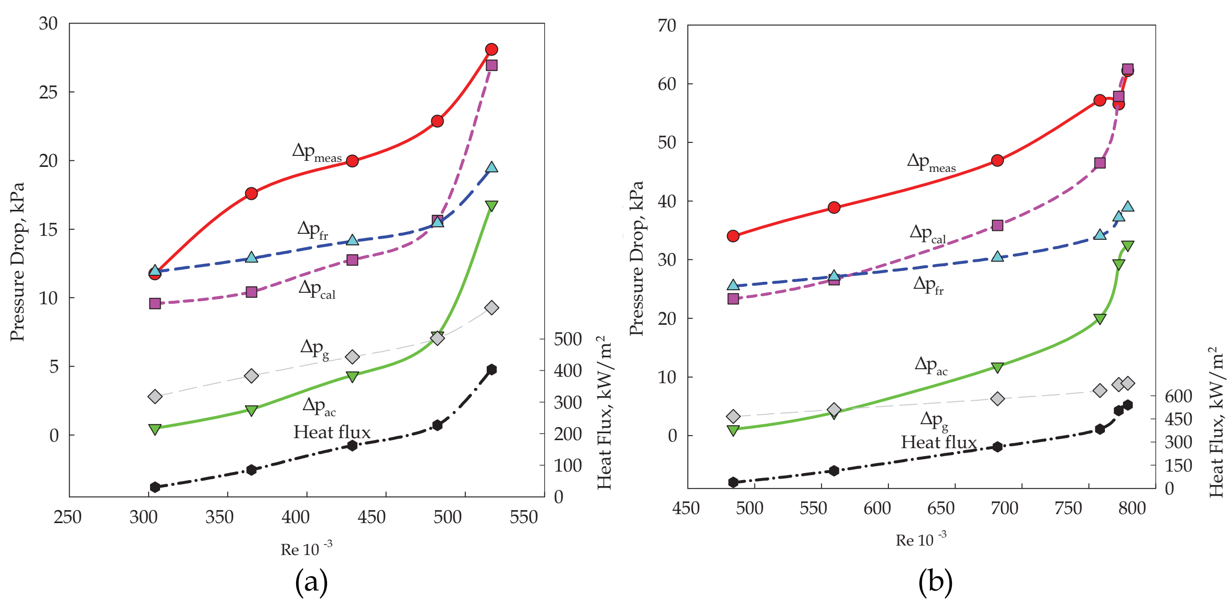

Fig. 15. Effect of Reynolds number on total pressure drop (measured and calculated) and its components (calculated values) in supercritical carbon dioxide flowing in vertical circular tube: p_{out}=8.8 MPa; (a) G=2040 kg/m²s, t_{in}=32ºC; and (b) G=3040 kg/m²s, t_{in}=31ºC.

In general, two major approaches to solve this problem were taken: an analytical approach (including numerical approach) and an experimental (empirical) approach.
Unfortunately, satisfactory analytical and numerical methods have not yet been developed, due to the difficulty in dealing with the steep property variations, especially in turbulent flows and at high heat fluxes. Therefore, empirical correlations are usually used.
For reference purposes, selected results obtained at Chalk River Laboratories (Pioro and Duffey, 2007; Pioro et al. 2004) are shown in Fig. 15. In these experiments, the local pressure drop due to obstructions along the heated length was 0, because of a smooth test section. Therefore, the measured pressure drop consists only of three components:

$$\Delta p_{meas} = \Delta p_{fr} + \Delta p_{ac} + \Delta p_g \,. \tag{17}$$

Other details of pressure drop at supercritical pressures are listed in Pioro and Duffey (2007).
Another important issue at supercritical and subcritical pressures is uncertainties of measured and calculated parameters. Pioro and Duffey (2007) dedicated a separate Appendix D to this important issue in their book.

6. Nomenclature

A	flow area, m^2
c_p	specific heat at constant pressure, J/kg K
$\bar{c}_p$	averaged specific heat within the range of (t_w – t_b); $\left(\dfrac{H_w - H_b}{T_w - T_b}\right)$, J/kg K
D	inside diameter, m
G	mass flux, kg/m^{2}s; $\left(\dfrac{m}{A_{fl}}\right)$
g	gravitational acceleration, m/s^2
H	specific enthalpy, J/kg
h	heat transfer coefficient, W/m^{2}K
k	thermal conductivity, W/m K
L	heated length, m
m	mass-flow rate, kg/s; $(\rho\, V)$
P, p	pressure, MPa
Q	heat-transfer rate, W
q	heat flux, W/m^2; $\left(\dfrac{Q}{A_h}\right)$
T, t	temperature, °C
u	axial velocity, m/s
V	volume-flow rate, m^3/kg
x	axial coordinate, m

Greek letters

a	thermal diffusivity, m^2/s; $\left(\dfrac{k}{c_p\, \rho}\right)$

Δ difference
θ test-section inclination angle, degree
μ dynamic viscosity, Pa s
ξ friction coefficient
ρ density, kg/m^3
υ kinematic viscosity, m^2/s

Non-dimensional numbers

Nu Nusselt number; $\left(\frac{h\,D}{k}\right)$

Pr Prandtl number; $\left(\frac{\mu\,c_p}{k}\right)=\left(\frac{\upsilon}{\alpha}\right)$

$\overline{\mathrm{Pr}}$ averaged Prandtl number within the range of (t_w – t_b); $\left(\frac{\mu\ \bar{c}_p}{k}\right)$

Re Reynolds number; $\left(\frac{G\,D}{\mu}\right)$

Symbols with an overbar at the top denote average or mean values (e.g., $\overline{\mathrm{Nu}}$ denotes average (mean) Nusselt number).

Subscripts or superscripts

ac acceleration
ave average
b bulk
cal calculated
cr critical
dht deteriorated heat transfer
exp experimental
fl flow
fr friction
g gravitational
h heated
hy hydraulic-equivalent
in inlet
ℓ local
meas measured
out outlet or outside
pc pseudocritical
w wall

Abbreviations and acronyms widely used in the text

DHT Deteriorated Heat Transfer
GIF Generation-IV International Forum
HT Heat Transfer
HTC Heat Transfer Coefficient
ID Inside Diameter
IHT Improved Heat Transfer
NHT Normal Heat Transfer

NIST National Institute of Standards and Technology (USA)
SCWR SuperCritical Water-cooled Reactor

7. Reference

Ackerman, J.W., 1970. Pseudoboiling heat transfer to supercritical pressure water in smooth and ribbed tubes, Journal of Heat Transfer, Transactions of the ASME, 92 (3), pp. 490–498, (Paper No. 69-WA/HT-2, pp. 1–8).

Bishop, A.A., Sandberg, R.O., and Tong, L.S., 1965, Forced Convection Heat Transfer to Water at Near-critical Temperatures and Supercritical Pressures, *A.I.Ch.E.-I.Chem.E Symposium Series No*. 2, pp. 77−85.

Bishop, A.A., Sandberg, R.O. and Tong, L.S., 1964. Forced convection heat transfer to water at near-critical temperatures and super-critical pressures, Report WCAP-2056, Westinghouse Electric Corporation, Atomic Power Division, Pittsburgh, PA, USA, December, 85 pages.

Cheng, X., Yang, Y.H., and Huang, S.F., 2009, A Simple Heat Transfer Correlation for SC Fluid Flow in Circular Tubes, (NURETH-13), Kanazawa City, Ishikawa Prefecture, Japan, September 27-October 2.

Dittus, F.W. and Boelter, L.M.K., 1930. University of California, Berkeley, Publications on Engineering, Vol. 2, p. 443.

Dyadyakin, B.V. and Popov, A.S., 1977. Heat transfer and thermal resistance of tight seven-rod bundle, cooled with water flow at supercritical pressures, (In Russian), Transactions of VTI (Труды ВТИ), No. 11, pp. 244–253.

Filonenko, G.K., 1954. Hydraulic resistance of pipelines, (In Russian), Thermal Engineering, No. 4, pp. 40–44.

Gnielinski, V., 1976, New Equation for Heat and Mass Transfer in Turbulent Pipe and Channel Flow, *Intern. Chem. Eng.*, Vol. 16, No. 2, pp. 359-366.

Griem, H., 1996, A New Procedure for the at Near-and Supercritical Prediction Pressure of Forced Convection Heat Transfer, *Heat Mass Trans.*, Vol. 3, pp. 301–305.

Hadaller, G. and Banerjee, S., 1969, Heat Transfer to Superheated Steam in Round Tubes, AECL Report.

Jackson, J.D., 2002. Consideration of the heat transfer properties of supercritical pressure water in connection with the cooling of advanced nuclear reactors, Proceedings of the 13th Pacific Basin Nuclear Conference, Shenzhen City, China, October 21–25.

Kafengauz, N.L., 1986. About some peculiarities in fluid behaviour at supercritical pressure in conditions of intensive heat transfer, Applied Thermal Sciences, (Промышленная Теплотехника, стр. 6–10), 8 (5), pp. 26–28.

Kafengaus, N.L., 1975. The mechanism of pseudoboiling, Heat Transfer-Soviet Research, 7 (4), pp. 94–100.

Kirillov, P.L., Lozhkin, V.V. and Smirnov, A.M., 2003. Investigation of borders of deteriorated regimes of a channel at supercritical pressures, (In Russian), State Scientific Center of Russian Federation Institute of Physics and Power Engineering by the name of A.I. Leypunskiy, FEI-2988, Obninsk, Russia, 20 pages.

Krasnoshchekov, E.A., Protopopov, V.S., Van, F. and Kuraeva, I.V., 1967. Experimental investigation of heat transfer for carbon dioxide in the supercritical region, Proceedings of the 2nd All-Soviet Union Conference on Heat and Mass Transfer, Minsk, Belarus', May, 1964, Published as Rand Report R-451-PR, Edited by C. Gazley, Jr., J.P. Hartnett and E.R.C. Ecker, Vol. 1, pp. 26–35.

Krasyakova, L.Yu., Raykin, Ya.M., Belyakov, I.I. et al., 1967. Investigation of temperature regime of heated tubes at supercritical pressure, (In Russian), Soviet Energy Technology (Энергомашиностроение), No. 1, pp. 1–4.

Kuang, B., Zhang, Y., and Cheng, X., 2008, A New, Wide-Ranged Heat Transfer Correlation of Water at Supercritical Pressures in Vertical Upward Ducts, NUTHOS-7, Seoul, Korea, October 5–9.

Lee, R.A. and Haller, K.H., 1974. Supercritical water heat transfer developments and applications, Proc. 5th International Heat Transfer Conference, Tokyo, Japan, September 3–7, Vol. IV, Paper No. B7.7, pp. 335–339.

McAdams, W.H., 1942. Heat Transmission, 2nd edition, McGraw-Hill, New York, NY, USA, 459 pages.

Mokry, S., Farah, A., King, K., Gupta, S., Pioro, I. and Kirillov, P., 2009. Development of Supercritical Water Heat-Transfer Correlation for Vertical Bare Tubes, Proceedings of the Nuclear Energy for New Europe 2009 International Conference, Bled, Slovenia, 2009 September 14 – 17, Paper #210, 13 pages.

National Institute of Standards and Technology, 2007. NIST Reference Fluid Thermodynamic and Transport Properties-REFPROP. NIST Standard Reference Database 23, Ver. 8.0. Boulder, CO, U.S.: Department of Commerce.

Ornatskiy, A.P., Dashkiev, Yu.G. and Perkov, V.G., 1980. Supercritical Steam Generators, (In Russian), VyshchaShkola Publishing House, Kiev, Ukraine, 287 pages.

Pioro, I., Duffey, R. and Dumouchel, T., 2004. Hydraulic resistance of fluids flowing in channels at supercritical pressures (survey), Nuclear Engineering and Design, 231 (2), pp. 187–197.

Pioro, I.L. and Duffey, R.B., 2007. Heat Transfer and Hydraulic Resistance at Supercritical Pressures in Power Engineering Applications, ASME Press, New York, NY, USA, 328 pages.

Razumovskiy, V.G., 2003. Private communications, State Technical University "KPI", Kiev, Ukraine.

Richards, G., Milner, A., Pascoe, C. et al., 2010. Heat Transfer in a Vertical 7-Element Bundle Cooled with Supercritical Freon-12, Proc. 2nd Canada-China Joint Workshop on Supercritical Water-Cooled Reactors (CCSC-2010), Toronto, Ontario, Canada, April 25-28, 10 pages.

Seider, N. M., and Tate, G. E., 1936, Heat Transfer and Pressure Drop of Liquids in Tubes, *Ind. Eng. Chem.* 28 (12), pp. 1429–1435.

Shiralkar, B.S. and Griffith, P., 1970. The effect of swirl, inlet conditions, flow direction, and tube diameter on the heat transfer to fluids at supercritical pressure, Journal of Heat Transfer, Transactions of the ASME, 92 (3), August, pp. 465–474.

Swenson,H.S., Carver, J.R. and Kakarala, C.R., 1965.Heat transfer to supercritical water in smooth-bore tubes, Journal of Heat Transfer, Transactions of the ASME, Series C, 87 (4), 1965, pp. 477–484.

Styrikovich, M.A., Margulova, T.Kh. and Miropol'skii, Z.L., 1967. Problems in the development of designs of supercritical boilers, Thermal Engineering (Теплоэнергетика, стр. 4–7), 14 (6), pp. 5–9.

Vanyukova, G.V., Kuznetsov, Yu.N., Loninov, A.Ya., Papandin, M.V., Smirnov, V.P. and Pioro, I.L., 2009. Application of CFD-Code to Calculations of Heat Transfer in a Fuel Bundle of SCW Pressure-Channel Reactor, Proc. 4th Int. Symp.on Supercritical Water-Cooled Reactors, March 8-11, Heidelberg, Germany, Paper No. 28, 9 pages.

Vikhrev, Yu.V., Barulin, Yu.D. and Kon'kov, A.S., 1967. A study of heat transfer in vertical tubes at supercritical pressures, Thermal Engineering (Теплоэнергетика, стр. 80–82), 14 (9), pp. 116–119.

Vikhrev, Yu.V.,Kon'kov, A.S., Lokshin, V.A. et al., 1971. Temperature regime of steam generating tubes at supercritical pressure, (In Russian), Transactions of the IVth All-Union Conference on Heat Transfer and Hydraulics at Movement of Two-Phase Flow inside Elements of Power Engineering Machines and Apparatuses, Leningrad, Russia, pp. 21–40.

Watts, M. J., and Chou, C-T., 1982, Mixed Convection Heat Transfer to Supercritical Pressure Water, Proc. 7th International Heat Transfer Conference, Munich, Germany, pp. 495–500.

Yamagata, K., Nishikawa, K., Hasegawa, S. et al., 1972. Forced convective heat transfer to supercritical water flowing in tubes, International Journal of Heat & Mass Transfer, 15 (12), pp. 2575–2593.

Zahlan, H., Groeneveld, D., & Tavoularis, S. (April 25-28, 2010). Look-Up Table for Trans-Critical Heat Transfer. The 2nd Canada-China Joint Workshop on Supercritical Water-Cooled Reactors (CCSC-2010). Toronto, Ontario, Canada: Canadian Nuclear Society.

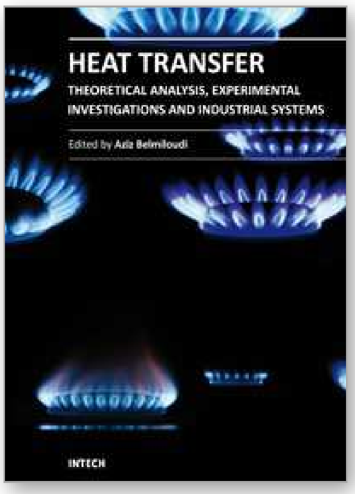

Heat Transfer - Theoretical Analysis, Experimental Investigations and Industrial Systems

Edited by Prof. Aziz Belmiloudi

ISBN 978-953-307-226-5
Hard cover, 654 pages
Publisher InTech
Published online 28, January, 2011
Published in print edition January, 2011

Over the past few decades there has been a prolific increase in research and development in area of heat transfer, heat exchangers and their associated technologies. This book is a collection of current research in the above mentioned areas and discusses experimental, theoretical and calculation approaches and industrial utilizations with modern ideas and methods to study heat transfer for single and multiphase systems. The topics considered include various basic concepts of heat transfer, the fundamental modes of heat transfer (namely conduction, convection and radiation), thermophysical properties, condensation, boiling, freezing, innovative experiments, measurement analysis, theoretical models and simulations, with many real-world problems and important modern applications. The book is divided in four sections : "Heat Transfer in Micro Systems", "Boiling, Freezing and Condensation Heat Transfer", "Heat Transfer and its Assessment", "Heat Transfer Calculations", and each section discusses a wide variety of techniques, methods and applications in accordance with the subjects. The combination of theoretical and experimental investigations with many important practical applications of current interest will make this book of interest to researchers, scientists, engineers and graduate students, who make use of experimental and theoretical investigations, assessment and enhancement techniques in this multidisciplinary field as well as to researchers in mathematical modelling, computer simulations and information sciences, who make use of experimental and theoretical investigations as a means of critical assessment of models and results derived from advanced numerical simulations and improvement of the developed models and numerical methods.

Phone: +385 (51) 770 447
Fax: +385 (51) 686 166
www.intechopen.com

Phone: +86-21-62489820
Fax: +86-21-62489821